



## Techno-economic feasibility of wind-powered reverse osmosis brackish water desalination systems in southern Algeria

Z. Triki<sup>a,\*</sup>, M. N. Bouaziz<sup>a</sup>, M. Boumaza<sup>b</sup>

<sup>a</sup>Laboratory of Biomaterials and Transport Phenomena (LBMP), Department of Process and Environmental Engineering, University of Médéa, Médéa, Algeria

Tel. + 213 (0) 25588466; Fax: + 213 (0) 25581253; email: triki.zakaria@univ-medea.dz

<sup>b</sup>Department of Chemical Engineering, College of Engineering, King Saud University, Riyadh, Saudi Arabia

Received 1 December 2011; Accepted 2 April 2013

---

### ABSTRACT

Water desalination is one of the most important factors that can help in developing remote areas and the desert. A critical technical parameter of desalination applications is the way the system is powered. This decision is taken according to the selected method of desalination and the characteristics of the candidate area. Nowadays, the method of reverse osmosis dominates globally; it requires only electricity, has a quite low specific energy demand, and can cooperate with technologies of renewable energy sources such as wind turbine and photovoltaics. Hence, renewable energy-powered reverse osmosis systems are promising technologies for brackish and seawater desalination in remote regions as they exhibit low energy consumption and can be designed according to water demand and energy resource. This study analyzes the feasibility of using wind energy to power brackish water reverse osmosis desalination units proposed for the development of the southern region of the case study country of Algeria. A reverse osmosis desalination scheme powered by a stand-alone wind turbine of 1 MW rated power is presented to elucidate its feasibility. The modeling results show that at average wind speeds, the amount of product water is sufficient to meet freshwater demand in this region. The effect of different operating and design conditions on the purified water production rate was investigated. The paper is concluded with the economic feasibility of wind-desalination systems at the selected sites.

*Keywords:* Remote areas; Brackish groundwater; Renewable energy sources; Wind power; Reverse osmosis desalination; Energy recovery

---

### 1. Introduction

Desalination of brackish and seawater has become one of the most widely applicable methods to meet

water demand and it is today widely applied in areas with limited water resources. However, because desalination is an energy-intensive process, energy cost has been the greatest barrier to its development. Among all the desalination process technologies, reverse osmosis (RO) has demonstrated the highest

---

\*Corresponding author.

electrical energy efficiency. Advantages in membrane technology and energy recovery devices (ERD) have led to a relatively low specific energy consumption (SEC) of RO processes to around 2–4 kWh/m<sup>3</sup> [1,2]. Even so, energy cost accounts for about 40% of total desalinated water cost by RO. From both an energy cost and an environmental point of view, inexpensive and clean alternative power sources are then needed to provide a low-cost desalination solution.

Wind-powered desalination is one of the most promising alternatives of renewable energy desalination. It can be competitive with other desalination systems, providing safe and clean drinking water efficiently in an environmentally responsible manner [3,4]. Several simulation studies show the feasibility of wind-powered desalination technologies, through the analysis of different types of membranes and feed-water quality levels. The main challenges associated with the use of wind turbines (WT) are the intermittency and fluctuations of the wind resource which occur due to turbulence and gusts over short periods of time (seconds to a few minutes) and mass air movements over long periods of time (tens to hundreds of hours) [5].

Different approaches for wind desalination systems are possible. First, both the WT as well as the desalination system are connected to a grid system (on-grid). In this case, the optimal sizes of the WT system and the desalination system as well as avoided fuel costs are of interest. The second option is based on a more or less direct coupling of the WT (s) and the desalination system (stand-alone). In this case, the desalination system is affected by power variations and interruptions caused by the power source (wind). These power variations, however, have an adverse effect on the performance and component life of certain desalination equipment. Hence, back-up systems, such as batteries, diesel generators, or flywheels might be integrated into the system [6]. Stand-alone systems can be a very good option in remote regions, where connection to the public electrical grid is either not cost-effective or not feasible, and where the water scarcity is severe.

A preliminary cost evaluation of wind-powered RO was presented by Garcia-Rodriguez et al. [7]. In particular, the influence of climatic conditions and plant capacity on product cost was analyzed for seawater RO driven by wind power. Additionally, the possible evolution of product cost due to possible future changes in wind power and RO technologies is evaluated. Finally, the influence on the competitiveness of wind-powered RO vs. conventional RO plants due to the evolution of financial parameters and cost of conventional energy was pointed out.

An analytical study of utilizing wind power for RO desalination was conducted by Kiranousdis et al. [8]. Generalized design curves for processing structural and operation variables were derived. The study indicated that the unit cost of freshwater production by a conventional RO plant could be reduced up to 20% for regions with an average wind speed of 5 m/s (measured at standard height, i.e. 10 m) or higher.

Miranda et al. [9] have employed a control strategy that attempts to maximize energy extracted and water throughput despite power fluctuations. They have developed and tested a small seawater RO unit driven by a 2.5 kW wind generator without batteries. The system operates at variable flow, enabling it to make efficient use of the naturally varying wind resource, without need of batteries.

Carta et al. [10] have presented a fully autonomous, battery-less system which consists of a wind farm supplying the energy needs of a group of eight RO modules. The main innovation of this system refers to the implementation of an automatic operation strategy, controlling the number of RO modules that have to be connected in order to match the variable wind energy supply.

Forstmeier et al. [4] have evaluated the economic feasibility of a wind-powered RO plant by mathematical modeling analysis. It was shown that the costs of a wind-powered RO desalination system are in line with what is expected for a conventional desalination system, proving to be particularly cost-competitive in areas with good wind resources that have high costs of energy.

Zejli et al. [11] have investigated the economic feasibility of a 11 MW wind-powered RO desalination system connected to the grid in the Tan-Tan town (Morocco) by the assessment of the levelized cost of fresh water. The research found that the proposed system is not economically feasible in this town to its low wind potential.

Park et al. [12] have tested a wind-powered reverse osmosis membrane system without energy storage using synthetic brackish water over a range of simulated wind speeds under both steady-state and fluctuating conditions. The main challenge associated with operation of this nature is the effect of the power switching off which causes reduced flux and permeate quality. This work has demonstrated that membrane systems can be directly connected to renewable energy systems (wind power presents the most extreme fluctuations) and operate effectively within a safe operating window with large power fluctuations, but further control strategies are required to deal with intermittent operation, especially with higher salinity feedwaters.

Recently, Käufler et al. [1] have presented the technical and economic specifications for wind powered seawater desalination with RO by the levelized water cost for typical plant configurations and relevant parameter variations. They revealed that the grid tariff is the significant criteria for the economic viability/application areas of wind powered vs. conventional processing since conventional grid power is intended to be replaced by wind power.

This study explores the feasibility of wind-desalination concepts in southern Algeria, and evaluates their economic viability. A RO desalination system powered by a stand-alone WT of 1 MW rated power was proposed to supply fresh water to the rural world of three potentially high-wind sites in the southwest of Algeria [13], namely Adrar, Timimoun, and Tindouf. A mathematical model based on the solution–diffusion theory and multiple fouling mechanisms was developed to simulate the process under steady-state conditions. The influence of operating parameters such as wind speed, transmembrane pressure, water recovery, and feed flow rate on the system performance was established. The paper is concluded with the economic viability of wind-powered desalination systems for the presented case.

## 2. Sites description

Algeria has a vast uninhabited land area where the south (desert) represents the greatest part with considerable wind regime. The Algerian wind map related to measured data at 10 m above ground level (a.g.l) shows that the best wind energy potential is in the southwestern region (Adrar, Timimoun, and Tindouf) where the average wind velocity is higher than 5–6 m/s as seen in Fig. 1. According to a recent review by Himri et al. [14] on the sites used in this study, wind farms of 30 MW installed capacity at Adrar, Timimoun, and Tindouf, if developed, could produce respectively 98,832, 78,138, and 56,040 MWh of electricity annually which demonstrate high potential for great wind energy harvest. The latitude, longitude, altitude, and the annual mean wind speeds of the three locations are summarized in Table 1 [14,15].

Besides, Algeria disposes of a considerable amount of underground brackish water in the septentrional Sahara. There are two types of resources: the renewable resources, which are localized in the Hoggar-Tassili and Bechar-Tindouf valleys and the nonrenewable resources, which are contained in huge reservoirs of the two sedimentary basins: the Continental Intercalary and the Complex Terminal aquifers as shown in Fig. 2 [16]. Lack of fresh water supply represents one of the major constraints to development of such areas.

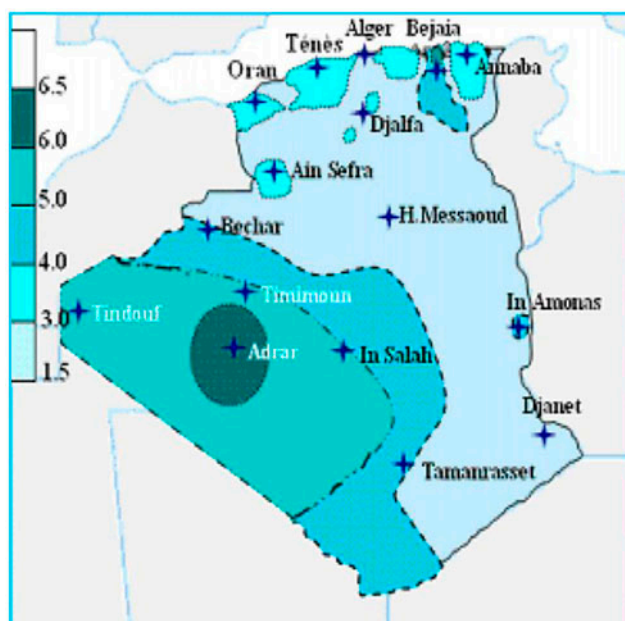


Fig. 1. Wind map evaluation in Algeria [14].

Table 1  
Geographical data for the selected sites

Sites	Latitude (deg)	Longitude (deg)	Altitude (m)	Annual mean wind speed (m/s)
Adrar	27°49'N	00°17' E	263	6.3
Timimoun	29°15'N	00°17' E	312	5.8
Tindouf	27°40'N	08°06' W	401	5.1

The presence of brackish water of moderate salinity (2,000–3,000 ppm) in some of these areas can present an economic and reliable fresh water supply, if an appropriate desalination scheme is adopted [17].

The selected sites are not very developed. This is due to their remoteness and to the harsh climatic conditions characterized by rigorous winters and torrid summers. Rain fall is rare and seldom exceeds 200 mm a year which increases water demands [18]. These regions are also scarcely populated. The dwellings, concentrated in scattered oases, are characterized by their isolated locations and their remoteness from any communication network. The sustainable development of the above regions requires then the introduction of an energy system that meets the need of the local population.

## 3. System description

The proposed system (Fig. 3) comprises a 1,000 kW WT (1) directly supplying a two-stage RO desalination unit with energy recovery and the option of interstage

pumping to boost pressure in the second stage. This two-staged layout is particularly suitable for brackish water desalination by reverse osmosis (BWRO) because the second-stage operation is favored by the remaining pressure of the first concentrate, thus allowing to increase the recovery rate and to reduce the pumping needs [19], however, increasing the membrane consumption for the process and this should be compensated via a framework in the literature [20]. The RO unit consists of pressure vessels (PVs) (8) in a two-stage array. PVs are arranged in parallel to satisfy the membranes flow and pressure specifications as well as

the plant production requirements. The total number of membranes and PVs required depends on permeate flow and applied pressure.

A feedwater supply pump (6) provides sufficient feed flow and pressure to the inlet of the main high pressure pump (HPP) (7) and pressure exchanger (PX) (10). The reject brine from the RO membranes passes into the PX, where its pressure and flow are transferred directly to a portion of the feedwater. The PX booster pump (9) is required to circulate the flow through the HP circuit. In traditional single-stage seawater designs, the booster pump is applied at the outlet of the PX. However, there is an opportunity for optimization in a second-stage brackish water design by applying the booster pump in between the first and second stages [21]. In this position, the PX booster pump also acts as an interstage booster pump to reduce the required pressure from the main HPP and help balance flux between the first and second stages. This booster pump location provides for an optimized isobaric energy recovery configuration for the BWRO process. Brine is discharged at atmospheric pressure.

As wind speed is highly variable, the flow rate and water pressure of the feedwater generated by the wind driven pump would also be highly variable. Therefore, adding a stabilizer and a feedback control mechanism (3) to adjust the flow rate and water pressure according to the variable wind speed would make the system more efficient. A temporary storage battery (2) is used to avoid energy fluctuations in the system and to enable continuous operation.

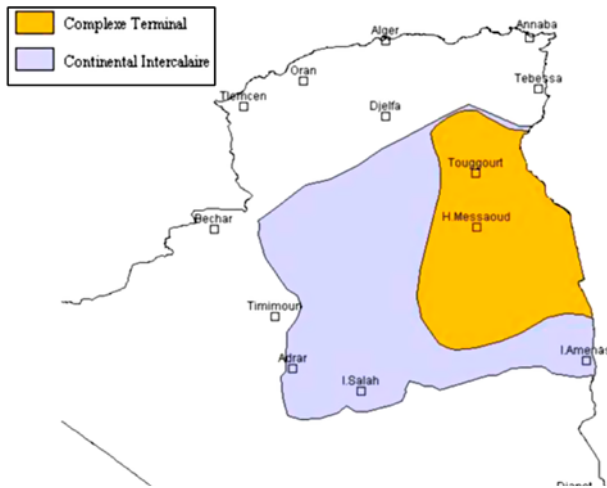


Fig. 2. Aquifer reservoirs in the south of Algeria [16].

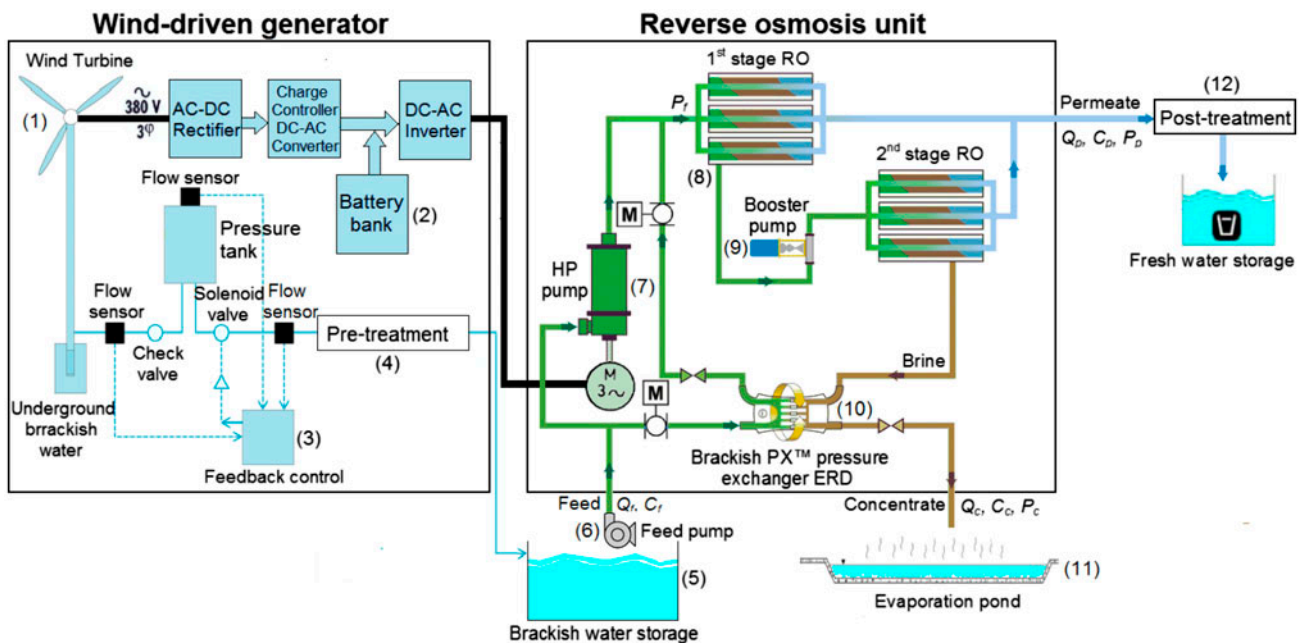


Fig. 3. Schematic of the wind-powered RO desalination system.

Feedwater pretreatment (4) is applied to maximize the RO system efficiency and membrane life by minimizing fouling, scaling, and membrane degradation. The degree of pretreatment depends on the quality of the feedwater, which to a large extent depends on the feedwater source. Brackish surface water typically has a greater propensity for membrane fouling and requires more extensive pretreatment systems than groundwater resources. Different methods should be carefully selected in order to cause minimum membrane fouling at the lowest possible cost. The amounts of chemicals added have to be precisely calculated depending on the scale forming salts contained in the feedwater. For water with low bacteria content, pretreatment may only require addition of polyelectrolyte as flocculation agent, and  $H_2SO_4$  to reduce the pH level and thus prevent  $CaCO_3$  precipitation. On the other hand, in the case of water with high bacteria content, more steps of chlorine addition and dechlorination should be included before the final stage consisting of sodium meta-sulfite dosing, activated carbon filtering, and ultra-violet treatment [22].

The desalination plant is connected to a water storage system (5) to ensure continuous operations in periods of reduced wind. This additional system is required because wind power varies with available winds, but most current desalination systems are currently designed to operate with consistent energy input.

The brine from the BWRO plant is fed to a series of evaporation ponds (11). This disposal system is especially effective in regions with low rainfall, and where climatic conditions are favorable for steady, and relatively rapid evaporation rates. By deploying such surfaces in arrays with large lateral dimensions, significant height and with minimal depth (e.g. 3–4 m), wind can be exploited to intensify evaporation for reduction of desalination brine volume [23].

Finally, a post-treatment process (12) is necessary before the water end-use. This may be achieved by injecting lime to increase the pH and chlorine for disinfection or by blending, with permeate, small amounts of filtered feedwater containing sufficient levels of calcium hardness and alkalinity [24].

## 4. Process modelling

### 4.1. Wind turbine energy output

The estimation of the wind power resources represents a major difficulty. Unlike the fossil fuel reserves, the quantity of the available energy varies with the season and the hour of the day. The availability of wind power is affected by the topography that solar energy. Moreover, the total quantity of convertible

wind power on the territory of a nation depends to a significant degree of the characteristics, the expected output, the design, and the layout of the WT field [25].

In order to calculate the average annual power from a WT over a range of mean wind speeds, a generalized expression is needed for the probability density distribution. Numerous studies in locations around the world have shown that the Weibull two-parameter distribution gives a good fit to wind data for wind energy applications [26]. The probability density of this distribution is given by:

$$f(V) = \left(\frac{k}{c}\right) \cdot \left(\frac{V}{c}\right)^{k-1} \times \exp\left[-\left(\frac{V}{c}\right)^k\right] \quad (1)$$

In this equation, the parameters,  $c$  and  $k$ , are used for fitting the distribution to a certain wind field.

In most cases, mean wind speed for a specific region is measured at a standard height (10 m a.g.l). In order to estimate the wind speed at different heights, the modified power law, developed by Mikhail and Justus [27], has been used:

$$c_2 = c_1 \times \left(\frac{Z_2}{Z_1}\right)^m \quad (2)$$

$$k_2 = \frac{k_1}{\left[1 - 0.0881 \cdot \ln\left(\frac{Z_2}{Z_1}\right)\right]} \quad (3)$$

The exponent,  $m$ , is a function depending on the roughness,  $Z_0$ , and the geometric height,  $Z$ , and is given by:

$$m = \frac{1}{\ln(Z/Z_0)} - 0.0881 \cdot \ln\left(\frac{c_1}{6}\right) \quad (4)$$

where:

$$Z = \sqrt{Z_1 \cdot Z_2} \quad (5)$$

The Weibull parameters for the frequency distribution at 10 m a.g.l are listed in the Table 2 for the selected locations [28].

The average annual power generated by the WT can be estimated using the following relation:

$$\bar{p} = \int_0^{\infty} p(V) \cdot f(V) \cdot dV \quad (6)$$

The turbine power curve  $p(V)$  is approximated by a quadratic equation in the range between the cut-in and rated speeds, as follows [29]:

Table 2  
Weibull wind speed distribution parameters

Site	Z <sub>0</sub> (m)	Weibull parameters	
		C <sub>1</sub> (m/s)	k <sub>1</sub> (–)
Adrar	0.01	7.2	2.15
Timimoun	0.01	6.5	1.91
Tindouf	0.01	5.8	1.85

$$p(V) = \begin{cases} 0 & \text{if } V < V_I \\ \alpha + \beta V + \gamma V^2 & \text{if } V_I \leq V < V_R \\ p_R & \text{if } V_R < V \leq V_O \\ 0 & \text{if } V > V_O \end{cases} \quad (7)$$

The constants  $\alpha$ ,  $\beta$ , and  $\gamma$  are determined under the following conditions:

$$\begin{cases} \alpha + \beta V_I + \gamma V_I^2 = 0 \\ \alpha + \beta V_R + \gamma V_R^2 = p_R \\ \alpha + \beta(V_I + V_R) + \gamma(V_I + V_R)^2 = p_R \left( \frac{V_I + V_R}{V_I} \right)^3 \end{cases} \quad (8)$$

Finally, Eq. (6) can be written as follows:

$$\bar{p} = \int_{V_I}^{V_O} (\alpha + \beta V + \gamma V^2) \frac{k_1}{c_1} \left( \frac{V}{c_1} \right)^{k_1-1} \exp \left[ - \left( \frac{V}{c_1} \right)^{k_1} \right] dV + p_R \left\{ \exp \left[ - \left( \frac{V_R}{c_1} \right)^{k_1} \right] - \exp \left[ - \left( \frac{V_O}{c_1} \right)^{k_1} \right] \right\} \quad (9)$$

The first term of this equation is a sample integration that can be easily solved numerically with Simpson’s rule.

Capacity factor or intermittence factor is one of the important indices for assessing the field performance of a WT. It is the ratio of the annual energy production, to the maximum theoretical energy production per year, i.e. running full time at rated power:

$$CF = \frac{\bar{p}}{p_R} \quad (10)$$

The annual electric power production of such a turbine is:

$$p_{aep} = \bar{p} \times (\text{time}) = (CF) \times p_R \times 8,760 \quad (11)$$

The WT-related parameters are summarized in Table 3 and the curve power is depicted in Fig. 4 [30].

Table 3  
Wind turbine parameters

Item	Value
Rated power (kW)	1,000
Rotor diameter (m)	54
Hub height (m)	70.82
Swept area of rotor (m <sup>2</sup> )	2,290
Cut-in wind speed (m/s)	3
Cut-out wind speed (m/s)	20
Rated wind speed (m/s)	16
Rotor speed (rpm)	15–22
Lifetime (yr)	25

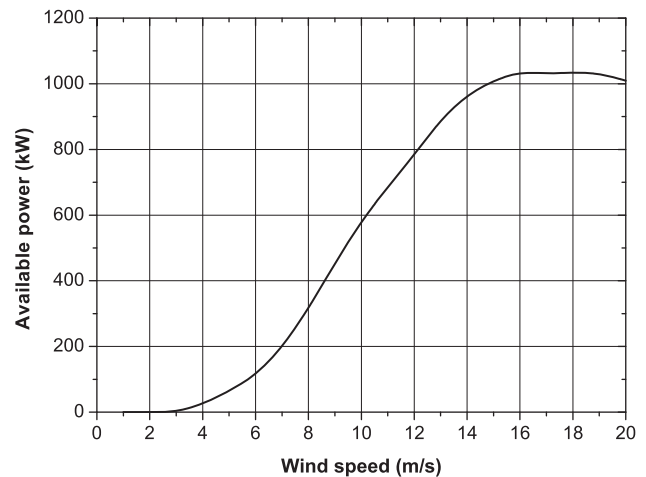


Fig. 4. Power curve of the wind turbine.

#### 4.2. RO desalination unit production

To estimate the unit production rate, it is assumed that diffusion type transport occurs through the membrane. As a result, the steady-state equations governing the transport of solvent and of solute are given as [31]:

$$Q_f = Q_c + Q_p \quad (12.a)$$

$$Q_f C_f = Q_c C_c + Q_p C_p \quad (12.b)$$

The volumetric flux of the solvent,  $J_w$ , is usually represented by [32]:

$$J_w = A(T)(\Delta P_f - \Delta \pi) \quad (13)$$

while the mass flux,  $J_s$ , of the solute is given by:

$$J_s = B(T)(C_m - C_p) \quad (14)$$

In the presence of concentration polarization at steady-state,  $J_w$ , is given by [33]:

$$J_w = k_s \ln \frac{C_m - C_p}{C_b - C_p} \quad (15)$$

We use:

$$\Delta\pi = b_\pi(C_m - C_p) \quad (16)$$

to estimate the osmotic pressure across the membrane, the solute flux can be written as follows:

$$J_s = J_w C_p \quad (17)$$

Combining Eqs. (14)–(16) (eliminating  $C_m$ ), we obtain, [34]:

$$J_w = A(T) \left[ \Delta P_f - b_\pi \left( C_b - \frac{B(T)C_b \exp(J_w/k_s)}{J_w + B(T) \exp(J_w/k_s)} \right) \exp(J_w/k_s) \right] \quad (18)$$

and

$$C_p = \frac{B(T)C_b}{B(T) + J_w \exp(J_w/k_s)} \quad (19)$$

Eq. (18) is an implicit nonlinear algebraic equation that can be solved numerically by the secant method. The value of the permeate concentration,  $C_p$ , can then be evaluated using Eq. (19). This concentration is constrained to lie below a desired value,  $C_{p,d}$ , such as:

$$C_p \leq C_{p,d} \quad (20)$$

Bulk concentration,  $C_b$ , is expressed as:

$$C_b = \frac{C_f + C_c}{2} \quad (21)$$

The effect of temperature on membrane water permeability,  $A(T)$ , and on membrane salts permeability,  $B(T)$ , are approximated by the following relations [35]:

$$A(T) = A_0 \frac{\mu(T_0)}{\mu(T)} \quad (22)$$

$$B(T) = B_0 \times \frac{T + 273.15}{T_0} \times \frac{\mu_0}{\mu(T)} \quad (23)$$

The effect of temperature on viscosity  $\mu(T)$ , is approximated by the Guzman–Andrade equation [36]:

$$\mu(T) = \alpha \exp\left(\frac{b}{T + 273.15}\right) \quad (24)$$

where  $\alpha = 7.142$  kg/m h and  $b = 1825.85$  K.

The recovery rate and the salt rejection are two parameters used to evaluate RO performance and are defined as:

$$R = \frac{Q_p}{Q_f} \quad (25)$$

$$SR = 1 - \frac{C_p}{C_b} \quad (26)$$

In spiral-wound membrane modules, perforated baffles are used, they increase mass transfer coefficient. For a channel containing baffle, the following equation is used to calculate mass transfer coefficient,  $k_s$  [37]:

$$Sh = 0.065 Re^{0.865} Sc^{0.25} \quad (27)$$

where:  $Sh = \frac{k_s d_h}{D_{AB}}$ ,  $Re = \frac{d_h u}{\nu}$  and  $Sc = \frac{\nu}{D_{AB}}$

Average velocity in the feed channel containing baffle is expressed as:

$$u = \frac{Q_b}{wh_{sp}\varepsilon} \quad (28)$$

where  $d_h$ ,  $h_{sp}$ , and  $\varepsilon$  are the baffle parameters.

Bulk flow rate of fluid is given by:

$$Q_b = \frac{Q_f + Q_c}{2} \quad (29)$$

In this paper, membrane modules constructed by Filmtec with trade name FILMTEC BW30–400 are chosen. The membranes are characterized by the stability of chemical, thermal, microbiological, and hydraulic resistance. Module’s specification and baffles’ dimensions and the specification of the membrane inside the module are given in Table 4 [38].

For brackish water, the kinematic viscosity,  $\nu$ , can be estimated from the following equation [39]:

$$\nu = 0.0032 + 3.0 \times 10^{-6} C + 4.0 \times 10^{-9} C^2 \quad (30)$$

The mass diffusivity,  $D_{AB}$ , is estimated as  $5.5 \times 10^{-6} \text{ m}^2/\text{h}$ .

Therefore, the osmotic coefficient,  $b_\pi$ , can be obtained as:

$$b_\pi = \frac{\pi}{C} \quad (31)$$

The osmotic pressure,  $\pi$ , is obtained from the below correlation:

$$\pi = 1,12T \sum \bar{m}_i \quad (32)$$

where  $\sum \bar{m}_i$  is the summation of molality of all of the dissolved ions.

The main physical chemical characteristics of the water of southern Algeria are given in Table 5 [40].

The energy required for the pressurization of the feed stream is calculated by means of the following equation:

$$p_{HPP} = \frac{Q_f \Delta P_f}{\eta_p} \quad (33)$$

The power recovered by the ERD is calculated as follows:

$$p_{ERD} = \Delta P_c Q_c \eta_{ERD} \quad (34)$$

Table 4  
Geometric specification of membrane module

Parameter	Value
Hydraulic diameter of channel (mm)	0.78045
Height of spacer channel (mm)	0.593
Void fraction of the spacer (porosity)	0.9
Length of membrane (m)	1
Width of membrane (m)	37
Active area of the membrane (m <sup>2</sup> )	37
Reference water permeability (m <sup>3</sup> /h.bar)	$19.43 \times 10^{-4}$
Reference solute permeability (m/h)	$78.55 \times 10^{-5}$

Table 5  
Characteristics of the brackish ground water

Item	Value
Temperature (°C)	20
Turbidity (NTU)	25
pH	6.5
Conductivity (ms/cm)	4.2
Na <sup>+</sup> (ppm)	460
K <sup>+</sup> (ppm)	45
Ca <sup>2+</sup> (ppm)	320
Mg <sup>2+</sup> (ppm)	135
F <sup>-</sup> (ppm)	3
Cl <sup>-</sup> (ppm)	1,140
SO <sub>4</sub> <sup>2-</sup> (ppm)	730
HCO <sub>3</sub> <sup>-</sup> (ppm)	100
TDS (ppm)	2,933

The pressure differential across the ERD at concentrate side is given by:

$$\Delta P_c = \Delta P_f - \Delta P_{drop} \quad (35)$$

The pressure drop,  $\Delta P_{drop}$ , is approximated by the correlation defined by Schock and Miquel [41]:

$$\Delta P_{drop} = \lambda \left( \frac{Q_f + Q_c}{2} \right)^\alpha \quad (36)$$

where:  $\alpha = 1.7$  and  $\lambda = 8.55 \times 10^{-3}$ .

The feed flow rate of water pumped by means of the WT can then be written as:

$$Q_f = \frac{3,600 \times \bar{p}}{\Delta P_f \eta_p^{-1} - [(1-R)(\Delta P_f - \lambda(Q_f(1-R/2))^\alpha) \eta_{ERD}]} \quad (37)$$

Eq. (37) is an implicit nonlinear algebraic equation that can be solved numerically. The Newton–Raphson method is used to solve this equation.

Finally, the specific energy consumption needed for the production of cubic meter of freshwater is given by:

$$SEC = \frac{\Delta P_f Q_f \eta_p^{-1} - \Delta P_c Q_c \eta_{ERD}}{Q_p} \quad (38)$$

## 5. Economic analysis

### 5.1. Cost estimation

The main parameters that influence the water production costs are [7]:

- plant capacity.
- climatic conditions, the characteristic of wind turbines, and the energy requirement of the RO plant.
- energy requirement of the desalination plant, which is determined by the salt concentration of the brackish water supply; the electric coupling of the wind-powered turbine and the RO module, the coupling of the ERD to the RO modules, and the properties of the membranes.
- the economic and financial parameters.

In this study, a levelized lifetime cost approach is used for the economic feasibility. This method takes into account all capital, operation and maintenance (O&M), and water costs. Transmission and distribution are not included. With these costs estimates and

appropriate values for the discount rate, technical lifetime, and plant capacity factor.

The levelized cost of energy (LEC), and the levelized cost of water (LWC), can be calculated as follow [42,43]:

$$LEC = \frac{Inv_{WT} \times A(n) + C_{aomWT}}{p_{aep}} \quad (39)$$

$$LWC = \frac{Inv \times A(n) + C_{aom}}{Q_p} \quad (40)$$

where:  $A(n) = \frac{i(i+1)^n}{(i+1)^n - 1}$ .

The present analyses are carried out using a discount rate,  $i$ , of 8%, over the assumed lifetime,  $n$ , of 25 years. The inflation is neglected and the land is offered by the state.

### 5.2. Profitability

Areas are determined economically feasible or infeasible based on two criteria: wind power classification and brackish groundwater desalination profitability. Wind energy can be feasible where the average wind velocity is higher than 5–6 m/s [44]. Profitability of desalination can be expressed in terms of profitability index (PI) or profit investment ratio defined as the ratio between the net present value (NPV) and the initial investment of the project [45]. Positive values of the PI indicate that the investment is viable while negative values indicate that the overall discounted costs are higher than the expected water selling price (WSP).

$$NPV = \frac{8,760 \times WSP \times Q_p - C_{aom}}{A(n)} - Inv \quad (41)$$

$$PI = \frac{NPV}{Inv} \quad (42)$$

The expected WSP is assumed to be 0.82 \$/m<sup>3</sup> based on grid electricity price (GEP) of 0.04 \$/kWh [46].

Table 6  
Capital and O&M costs

	Investment costs		O&M costs	
Wind	2,130	\$/kW	8	\$/ (MWh/yr)
Batteries	2,075	\$/kW	12	\$/ (MWh/yr)
Desalination	735	\$/ (m <sup>3</sup> /d)	0.14	\$/ (m <sup>3</sup> /yr)

The investment costs as well as the O&M costs used in economic study are given in Table 6 [47].

## 6. Results and discussion

### 6.1. Wind speed frequency distribution

The estimated wind speed frequencies obtained using the Weibull distribution are shown in Fig. 5 for the selected Algerian sites. The considered interval varies from 0 to 18 m/s. It can be seen that the location of Adrar has the maximum percentage of the wind speed above the 3 m/s cut-in wind speed, which contributes to the generation of electricity from wind. The location of Timimoun ranks second followed by Tindouf. This distribution shows that the higher average wind speeds generally correspond to the higher values of shape factor ( $k$ ). Small values of  $k$  imply that the data tend to be distributed over a relatively wide range of wind speeds.

### 6.2. System production

Table 7 gives the annual electricity production delivered by the WT and the daily nominal water production at the three sites. As can be seen from this table, the Adrar area with a yearly energy production of 3328.8 MWh represents the maximum power recovery. Timimoun and Tindouf area produce, respectively, an annual electric power of 2890.8 and 2452.8 MWh, respectively. Therefore, the higher capacity factor of 38% is obtained at Adrar followed by Timimoun and Tindouf (33–28%). Assuming that the daily operation time of the system is 24 h (use of batteries), this quantity of energy can produce 3,720 m<sup>3</sup>/d in Adrar, 3315.36 m<sup>3</sup>/d in Timimoun, and 2843.52 m<sup>3</sup>/d in Tindouf (modeling condition:  $R = 82\%$ ;  $\eta_p = 60\%$ ;  $\eta_{ERD} = 80\%$ ).

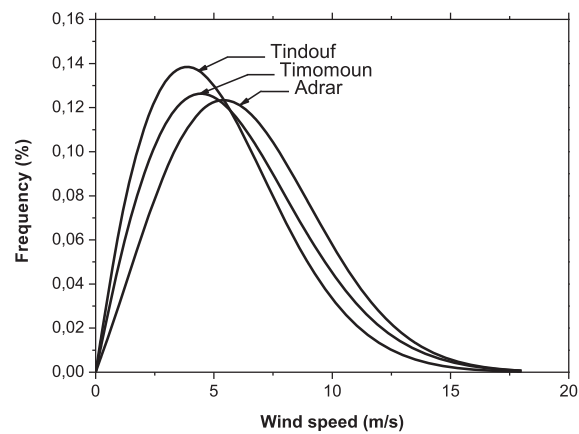


Fig. 5. Weibull distribution of the selected sites.

Table 7  
Energy and water productions for the selected sites

Sites	Annual energy production (MWh/yr)	Capacity factor (%)	Nominal production (m <sup>3</sup> /d)
Adrar	3,328.8	38	3,720
Timimoun	2,890.8	33	3,315.36
Tindouf	2,452.8	28	2,843.52

### 6.3. Sensitivity analyses

#### 6.3.1. Wind speed

The first analysis carried out aimed at establishing the input–output characteristic of the system. The relationship between wind speed and product flow rate is illustrated in Fig. (6a). Similarly to the WT power curve, it gives the expected output from the system. It can be seen that the production rate for the location of Adrar exceeds a capacity of 200 m<sup>3</sup>/h corresponding to a wind speed of 10 m/s.

The effect of the wind speed on the permeate concentration calculated for a production rate of 150 m<sup>3</sup>/h which is illustrated in Fig. (6b), shows that the salt concentration decreases as the wind speed increases and this is due to the increase in water pressure, as confirmed by Eqs. (18) and (19). However, it must be mentioned that, at high wind speeds, the trend of decrease in permeate concentration is relatively low and remains approximately constant. The reason is that when the operating pressure is near osmotic pressure, the quality of the permeate stream is low; thus an increase in the pressure affects the permeate quality rapidly. When the pressure is a little bit higher than osmotic pressure, the changes in permeate concentration is very small. It should be noted that for wind speed less than 8 m/s, the product water quality was insufficient for drinking water purposes (>500 ppm) and consequently was not considered in the above analysis.

#### 6.3.2. Water recovery

In Fig. (7a), the variations in specific energy and transmembrane pressure were shown for recovery ratio ( $R$ ) ranging from 10 to 90%. The feed pressure increases as the recovery ratio increases, indicating that higher pressure is required to obtain high recovery ratio. However, the specific energy decreases with increasing recovery ratio ranging from 10 to 60% and then increases with increasing recovery ratio over 60%. This is because the specific energy depends not

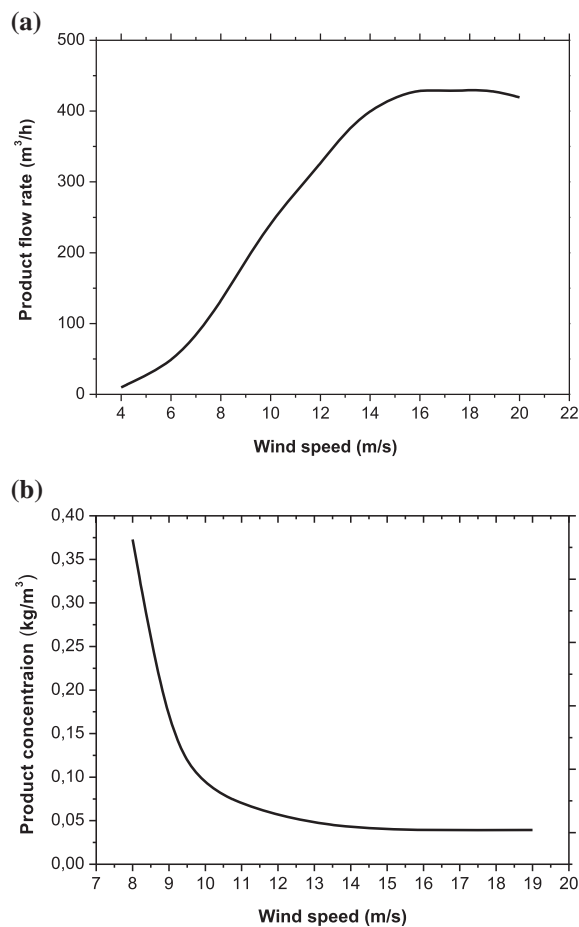


Fig. 6. Variation of the product flow rate and the permeate concentration with wind speed. Modeling condition:  $R = 82\%$ ;  $\eta_p = 60\%$ ;  $\eta_{ERD} = 80\%$  (Adrar).

only on the pressure difference across the membrane but also feed flow rate [see Eq. (38)]. As recovery increases, total energy consumption increases to obtain high pressure but less water can be pressurized to produce the required amount of product water, as shown in Fig. 7(b). Therefore, the specific energy, which is total energy consumption divided by feed flow rate, has a minimum value at an optimum recovery ratio. Under the given conditions, a minimum value for specific energy is 1.754 kWh/m<sup>3</sup> at  $R = 60\%$ . It must be stated that for SWRO, a minimum of SEC appears at a recovery ratio of about 40–55%, while the operating pressure is almost over 70 bar, depending on the feedwater salinity [48,49]. The need of such high pressures arises from the increased osmotic pressure of the feed with increased water recovery. Besides, a theoretical calculation of SEC at the limit of thermodynamic restriction [20,50] reveals that a minimum of SEC occurs at a recovery of exactly 50% in the absence of energy recovery and can be significant

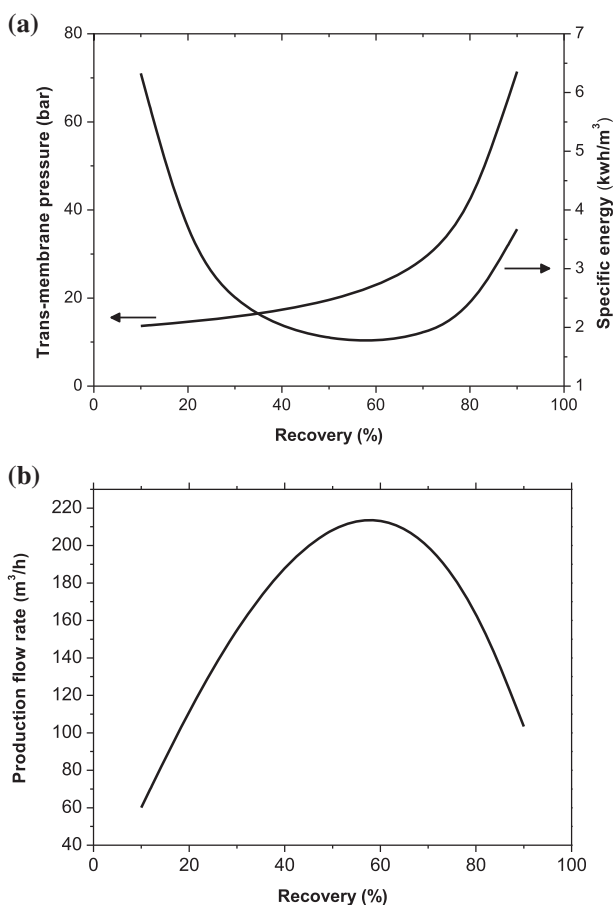


Fig. 7. Variation of the pressure, the specific energy and the production rate with recovery. Modeling condition:  $C_{pd} = 260$  ppm;  $\eta_p = 60\%$ ;  $\eta_{ERD} = 80\%$  (Adrar).

lower with the use of an ERD recoveries higher than 50% (40% lower specific energy for  $\eta_{ERD} = 80\%$  and  $\eta_p = 1$ ). As it is demonstrated, the deployment of an ERD shifts the optimal minimum energy location to lower recoveries; this appears in agreement with published results. According to an experimental study of the SEC for BWRO [51], a minimum of SEC may not necessarily exist for BWRO desalination. As it is explained, the concentration polarization across the membrane raises a barrier to the recovery ratio and might result to an optimum of specific energy; this effect is dominant for seawater RO process but not for brackish water.

### 6.3.3. Feed flow rate

Fig. 8(a and b) shows the effect of the feed flow rate on the system performance. As expected, increasing the feed flow rate will decrease the water recovery but increase both the water production rate and salt

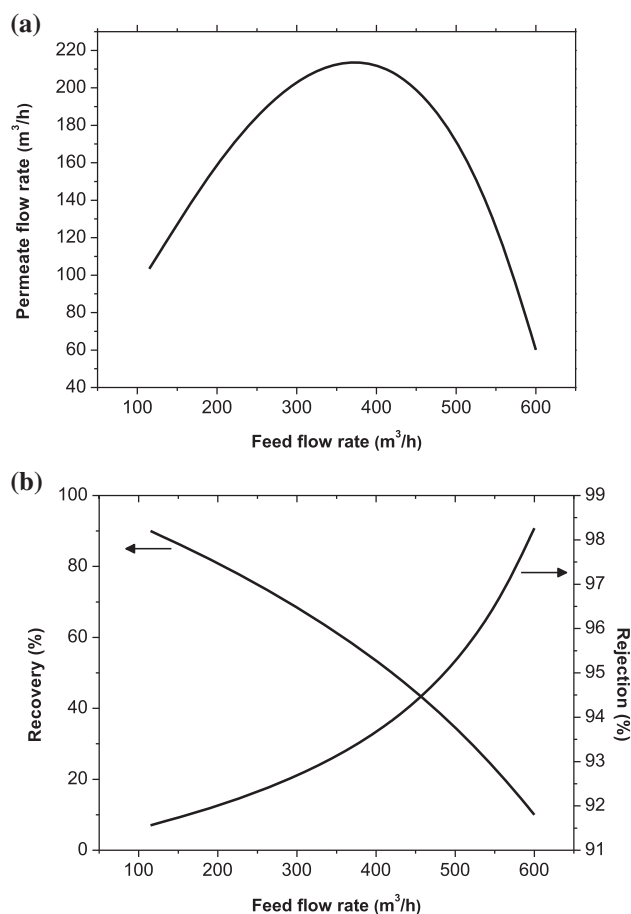


Fig. 8. Variation of the water recovery, salt rejection and production rate with feed flow rate. Modeling condition:  $C_{pd} = 260$  ppm;  $\eta_p = 60\%$ ;  $\eta_{ERD} = 80\%$  (Adrar).

rejection due the reduction in the average osmotic pressure. Therefore, it can be stated that higher feed flow rates lead to greater mass transfer coefficients due to reducing the effect of concentration polarization. The greater feed flow rates reduce salt concentration at the membrane surface therefore the average osmotic pressure reduces due to smaller salt concentrations. However, an increase of the feed rate above a certain optimum value will result in a reduction rather than an increase in the production rate, this phenomena is unexpected. The reason for the lower production rate is that the gain due to the lower average osmotic pressure is outweighed by the high frictional pressure drop, and hence, the net driving force is reduced. In other words, as the feed flow rate increase, the salt concentration on the feed brine side of the membrane increases, which causes an increase in salt flow rate across the membrane as indicated by Eq. (14). Also, a higher salt concentration in the feed stream increases the osmotic pressure, reducing the net driving

pressure and consequently reducing the product water flow rate according to Eq. (13). For specific given conditions, the maximum product flow rate which can be predicted is  $216.43 \text{ m}^3/\text{h}$  ( $Q_f=360.71 \text{ m}^3/\text{h}$ ).

6.3.4. Transmembrane pressure

The effect of the transmembrane pressure on the feed flow rate is shown in Fig. 9(a). It can be seen from this figure that higher membrane feed pressure results in a lower flow rate as predicted by Eq. (37). The effect of the transmembrane pressure on the salt rejection which is shown in Fig. 9(b), indicates that salt rejection increases nonlinearly with permeate flow rate and pressure as explained by Eq. (19). However, at relatively high pressures, the salt rejection decreases due to the rapid increase in the osmotic pressure as the brine progresses in the feed channel [52]. In other words, when the pressure increases over a critical value, as some salt will dissolve with water flowing through the membrane, the feed stream becomes more

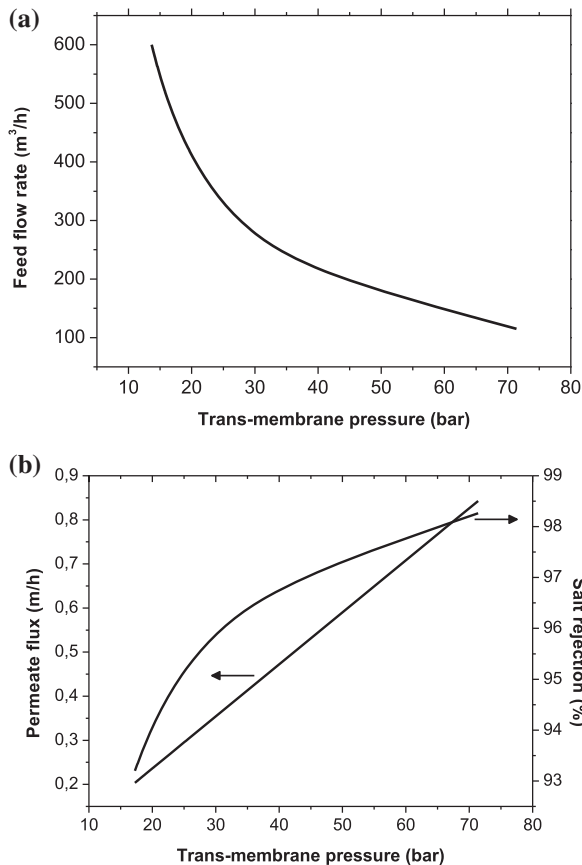


Fig. 9. Variation of the feed flow rate, the permeate flux and the salt rejection with pressure. Modeling condition:  $C_{pd} = 260 \text{ ppm}$ ;  $\eta_p = 60\%$ ;  $\eta_{ERD} = 80\%$  (Adrar).

concentrated which increases rapidly the osmotic pressure.

6.4. Economic feasibility

The results of energy and water costs calculation are shown in Fig. 10(a and b) for the three selected sites. The LEC is about  $0.14 \text{ \$/kWh}$  in Adrar,  $0.155 \text{ \$/kWh}$  in Timimoun, and  $0.18 \text{ \$/kWh}$  in Tindouf. The corresponding LWC is  $0.66$ ,  $0.7$ , and  $0.75 \text{ \$/m}^3$ , respectively. Obviously, the Adrar site presents the lowest LEC and LWC due to the higher annual electric power production. It must be mentioned that the obtained values of LEC are higher than the GEP if the price per kWh produced by the latter is set to  $0.04 \text{ \$/kWh}$ .

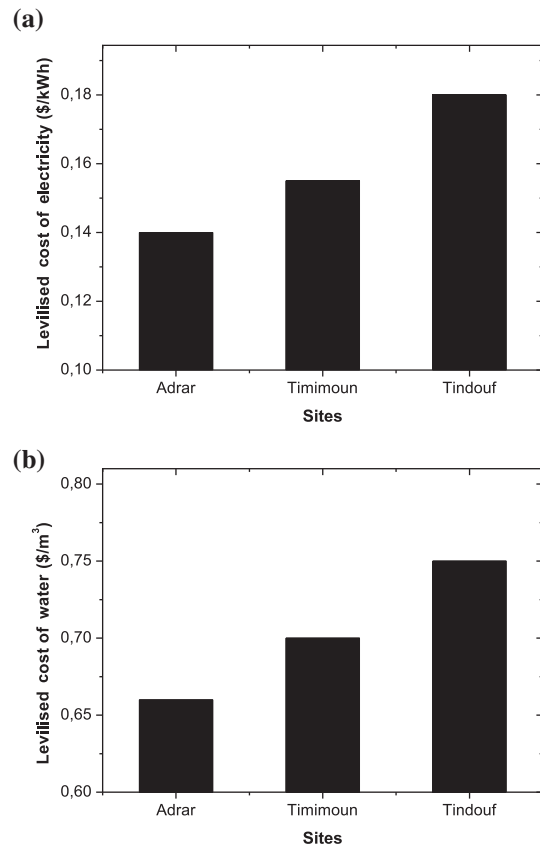


Fig. 10. LEC and LWC evaluation for the selected sites.

Table 8  
Economic feasibility indicators

Sites	Net present value (\$)	Profitability index (-)
Adrar	2,206,181	0.32
Timimoun	1,525,018	0.23
Tindouf	715,200.1	0.11

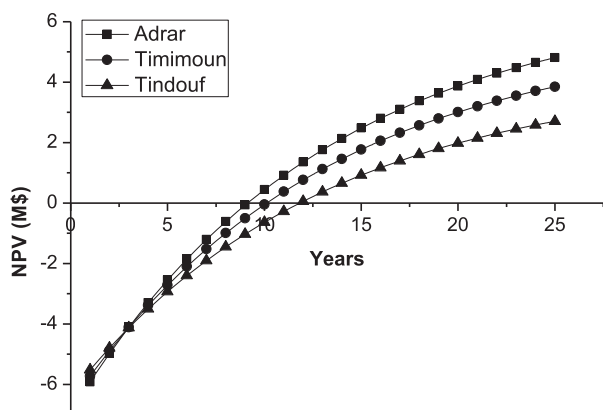


Fig. 11. NPV evaluation for the selected sites.

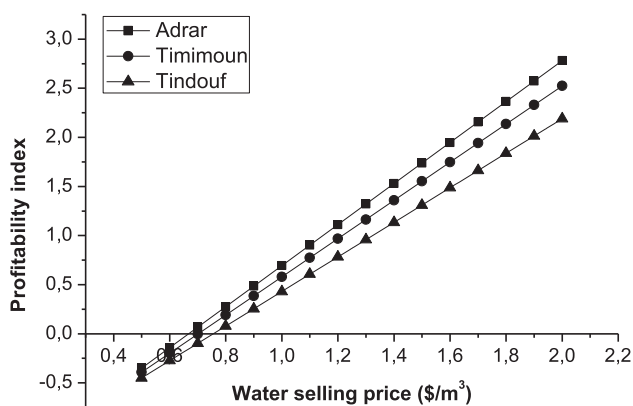


Fig. 12. PI as function of SWP for the selected sites.

kWh. This is due to high investment costs. However, the estimated LWC are lower than the current WSP (0.82 \$/m<sup>3</sup>).

The net present value evaluation of the studied hybrid desalination system is given in Table 8 for the three sites. The obtained NPV are 2,206,181\$, 1,525,018\$, and 715,200.1\$ at Adrar, Timimoun, and Tindouf, respectively, with corresponding profit investment ratios of 0.32, 0.23, and 0.11. The expected year-to-positive cash flow is 9 years in Adrar, 10 years in Timimoun, and 12 years in Tindouf as shown in Fig. 11.

Fig. 12 presents the PI as a function of the WSP for the selected sites. The graph is a straight line, in accordance with Eqs. (41) and (42). The slope of the line depends on the initial investment, the financing parameters of the investment (lifetime, discount rate), and the plant capacity. Higher slopes represent more attractive investments since a small increase of the WSP leads to a substantial increase of the PI and consequently to the NPV. Adrar is again considered the best site.

## 7. Conclusion

This study investigated the opportunity to use wind energy in three locations in the southern part of Algeria. With the scarcely populated regions, there is a vast land space for possible installation of wind farms for wind energy exploitation. It could provide a viable source of energy to power the BWRO desalination units which can help in the development of these regions. The results of the present study can be summarized as follows:

- The economic feasibility study based on the assumed economical parameters from the literature showed that wind-powered RO desalination seems to be a promising solution to provide power and fresh water supplies to remote areas in the south of Algeria.
- The annual electric power productions obtained using wind power curve of 1,000 kW at Adrar, Timimoun, and Tindouf were found to be 3,328.8, 2,890.8, and 2452.8 MWh, respectively. The plant capacity factors at these sites were found to be 38, 33, and 28% corresponding to nominal production capacities of 3,720, 3315.36, and 2843.52 m<sup>3</sup>/d.
- With a feedwater salinity of about 3,000 ppm, an average wind speed of 8 m/s or more was required to produce adequate-quality permeate ( $\leq 500$  ppm) for a product flow rate of 150 m<sup>3</sup>/h, i.e. 3,600 m<sup>3</sup>/d (Adrar region).
- The recovery ratio has to be optimized for low energy consumption and high permeate flux. Based on modeling results, the minimum specific energy was found to be 1.754 kWh/m<sup>3</sup> at optimum recovery ratio of 60% corresponding to a maximum production of 216.43 m<sup>3</sup>/h (Adrar region).
- Increasing the feed rate beyond a certain optimum value, the water production rate will decrease due to the reduction in the net transmembrane pressure difference resulting from the high frictional pressure drop.
- Increasing the feed flow rate increases salt rejection. The reason for this phenomenon is that higher feed flow rate increases mass transfer coefficient and concentration polarization parameter reaches unity.
- Increasing the operating pressure increases both the permeate flux and the salt rejection. However, increasing the pressure beyond a certain maximum value will lead to a deterioration of the quality of the product.
- The LWC was found to be 0.66 \$/m<sup>3</sup> at Adrar, 0.7 \$/m<sup>3</sup> at Timimoun, and 0.75 \$/m<sup>3</sup> at Tindouf while the LEC was found to vary in the range of 0.14–0.18 \$/kWh depending on the site. The high

values of LEC compared to the GEP (0.04\$/kWh) are due mainly to high O&M costs.

- The results of the economic study showed that positive cash flow could be obtained in 9, 10, and 12 years at Adrar, Timimoun, and Tindouf, respectively if the overall production cost of fresh water is set to 0.82\$/m<sup>3</sup>.
- The use of the PI could provide a tool for comparing the expected WSP to the current water consumption rates. This comparison represents one of the possible criteria in order to select the best option to cover the water needs of a specific region. The best options are those with small LWC and for which an increase of the WSP produces a large increase to the expected PI.

Finally, a more representative validation of the system will be only possible after prototype testing, which will provide a deeper understanding of the system performance, particularly considering the transients present in a system supplied by an extremely variable and unpredictable source, such as the wind.

### Symbols

$A_0$	— reference water permeability at 298 K (m/h bar)
$A(n)$	— capital recovery factor
$A(T)$	— temperature dependent water permeability (m/h bar)
$B(T)$	— temperature dependent solute permeability (m/h)
$B_0$	— reference solute permeability at 298 K (m/h)
$b_\pi$	— osmotic coefficient (m <sup>3</sup> bar/kg)
$c$	— scale factor (m/s)
$c_1$	— scale factor at 10 m a.g.l (m/s)
$c_2$	— scale factor at desired level (m/s)
$C$	— salt concentration (kg/m <sup>3</sup> )
$C_{aom}$	— total annual O&M costs (\$)
$C_{aomWT}$	— annual O&M costs of the wind turbine (\$)
$CF$	— capacity factor
$D_{AB}$	— mass diffusivity (m <sup>2</sup> /h)
$d_h$	— hydraulic diameter of channel (m)
$i$	— annual discount rate (%)
$Inv$	— total investment cost (\$)
$InvWT$	— investment cost of the wind turbine (\$)
$f(V)$	— weibull probability density function
$J_w$	— volumetric flux of water (m/h)
$J_s$	— salts mass flux (kg/m <sup>2</sup> h)
$k$	— shape factor (dimensionless)
$k_1$	— shape factor at 10 m a.g.l (dimensionless)
$k_2$	— shape factor at desired level (dimensionless)
$k_s$	— mass transfer coefficient (m/h)
$LEC$	— levelized cost of electricity (\$)

$LWC$	— levelized cost of water (\$)
$n$	— life time of the plant
$NPV$	— net present value (\$)
$p$	— power (W)
$P$	— pressure (bar)
$p_{aep}$	— annual electricity production from wind turbines (kWh/yr)
$PI$	— profitability index
$Q$	— volumetric flow rate (m <sup>3</sup> /h)
$Re$	— Reynolds number (dimensionless)
$Sc$	— Schmidt number (dimensionless)
$Sh$	— Sherwood number (dimensionless)
$R$	— recovery ratio (%)
$SEC$	— specific energy consumption (kWh/m <sup>3</sup> )
$SR$	— salt rejection (%)
$T$	— feedwater temperature (°C)
$T_0$	— reference water temperature equal to 298 K
$V$	— wind speed (m/s)
$u$	— velocity of water in feed channel (m/h)
$w$	— width of the membrane (m)
$WSP$	— water selling price (\$/m <sup>3</sup> )
$Z_0$	— roughness (m)
$Z$	— geometric height (m)
$Z_1$	— reference height (m)
$Z_2$	— desired height (m)

### Greek

$\Delta$	— difference
$\varepsilon$	— void fraction of the spacer (dimensionless)
$\eta$	— efficiency
$\mu_0$	— viscosity at 290 K (kg/m h)
$\mu(T)$	— temperature dependent viscosity (kg/m h)
$\nu$	— kinematic viscosity of salt solution (m <sup>2</sup> /h)
$\rho$	— water density (kg/m <sup>3</sup> )

### Subscripts

$b$	— bulk
$c$	— concentrate
$d$	— desired
$f$	— feed
$I$	— cut-in
$m$	— membrane
$O$	— cut-out
$p$	— permeate
$R$	— rated

### References

- [1] J. Käufler, R. Pohl, H. Sader, Seawater desalination (RO) as a wind powered industrial process—Technical and economical specifics, *Desalin. Water Treat.* 31 (2011) 359–365.
- [2] O.A. Hamed, A.M. Hassan, K. Al-Shail, M.A. Farooque, Performance analysis of a trihybrid NF/RO/MSF, *Desalin. Water Treat.* 1 (2009) 215–222.

- [3] S. Kalogirou, Seawater desalination using renewable energy sources, *Prog. Energy Combust. Sci.* 31 (2005) 242–281.
- [4] M. Forstmeier, F. Mannerheim, F. D'Amato, M. Shah, Y. Liu, M. Baldea, A. Stella, Feasibility study on wind-powered desalination, *Desalination* 203 (2007) 463–470.
- [5] D.A. Dehmasa, On the use of wind energy to power reverse osmosis desalination plant: A case study from Ténès (Algeria), *Renew. Sustain. Energy Rev.* 15 (2011) 956–963.
- [6] J.F. Manwell, J.G. McGowan, A.L. Rogers, *Wind energy explained-theory, design and application*, John Wiley & Sons Ltd, West Sussex, 2002.
- [7] L. Garcia-Rodriguez, V. Romero-Ternero, C. Gómez-Camacho, Economic analysis of wind-powered desalination, *Desalination* 137 (2000) 259–265.
- [8] C.T. Kiranoudis, N.G. Voros, Z.B. Maroulis, Wind energy exploitation for reverse osmosis desalination plants, *Desalination* 109 (1997) 195–209.
- [9] M.S. Miranda, D. Infield, A wind-powered seawater reverse-osmosis system without batteries, *Desalination* 153 (2002) 9–16.
- [10] J.A. Carta, J. Gonzalez, V. Subiela, Operational analysis of an innovative wind powered reverse osmosis system installed in Canary Islands, *Solar Energy* 75 (2003) 153–168.
- [11] D. Zejli, K.E. Aroui, A. Lazrak, K.E. Boury, A. Elmidaoui, Economic feasibility of a 11-MW wind powered reverse osmosis desalination system in Morocco, *Desalin. Water Treat.* 18 (2010) 164–174.
- [12] G.L. Park, A.I. Schäfer, B.S. Richards, Renewable energy powered membrane technology: The effect of wind speed fluctuations on the performance of a wind-powered membrane system for brackish water desalination, *J. Membr. Sci.* 370 (2011) 34–44.
- [13] R. Mitiche, M. Metaiche, A. Kettab, F. Ammour, S. Otmani, S. Houli, S. Taleb, A. Maazouzi, Desalination in Algeria, current situation and development program, *Desalin. Water Treat.* 14 (2010) 259–264.
- [14] Y. Himri, S. Rehman, B. Draoui, S. Himri, Wind power potential assessment for three locations in Algeria, *Renew. Sustain. Energy Rev.* 12 (2008) 2495–2504.
- [15] Y. Himri, A. Boudghene Stambouli, B. Draoui, S. Himri, Review of wind energy use in Algeria, *Renew. Sustain. Energy Rev.* 13 (2009) 910–914.
- [16] A. Fekraoui, F.Z. Kedaid, Geothermal resources and uses in Algeria: A country update report, *Proc. World Geothermal Congress*, Antalya, Turkey, April 2005, pp. 24–29.
- [17] B. Bouchekima, D. Bechki, H. Bouguettaia, S. Boughali, M.T. Meftah, The underground brackish waters in South Algeria: Potential and viable resources, *Proceedings of the 13th IWRA World Water Congress*, September 1–4, 2008, Montpellier, France.
- [18] R. Boudries, R. Dizene, Prospects of solar hydrogen production in the Adrar region, *Renewable Energy* 36 (2011) 2872–2877.
- [19] F. Vince, F. Marechal, E. Aoustin, P. Bréant, Multi-objective optimization of RO desalination plants, *Desalination* 222 (2008) 96–118.
- [20] A. Zhu, Effect of thermodynamic restriction on energy cost optimization of RO membrane water desalination, *Ind. Eng. Chem. Res.* 48 (2009) 6010–6021.
- [21] J.P. MacHarg, S.A. McClellan, Pressure exchanger helps reduce energy costs in brackish water RO system, *J. AWWA* 96 (2004) 44–48.
- [22] F. Morenski, Current pretreatment requirements for reverse osmosis membrane applications. *Proceedings of the 53rd International Water Conference*, Pittsburgh Hilton and Towers, October 19–21, 1992, pp. 325–330.
- [23] J. Gilron, Y. Folkman, R. Savliev, M. Waisman, O. Kedem, WAIV—wind aided intensified evaporation for reduction of desalination brine volum", *Desalination* 158 (2003) 205–214.
- [24] S. Walker, P. Mattausch, A. Abbott, Reverse osmosis treatment facilities: Innovative post-treatment stabilization solutions, *Florida Water Res. J.* 59(11) (2007) 35–37.
- [25] R. Maouedj, S. Bousalem, B. Benyoucef, Algeria wind energy resources, *Int. Sci. J. Altern. Energy Ecol.* 62(6) (2008) 155–162.
- [26] O.A. Jaramillo, M.A. Borja, Wind speed analysis in La Ventosa, Mexico: A bimodal probability distribution case, *Renewable Energy* 29 (2004) 1613–1630.
- [27] D. Poje, B. Cividini, Assessment of wind energy potential in Croatia, *Solar Energy* 41 (1988) 543–554.
- [28] N.K. Merzouk, Evaluation du gisement énergétique éolien contribution à la détermination du profil vertical de la vitesse du vent en Algérie, *Doctoral thesis*, University of Tlemcen, Algeria, May 2006.
- [29] B. Bagen, Reliability and Cost/Worth Evaluation of Generating Systems Utilizing Wind and Solar Energy. PhD Thesis, University of Saskatchewan Saskatoon, Saskatchewan, Canada, 2005.
- [30] <http://www.worldwidewindturbines.com/en/wind-turbines/wind-turbine-manufacturers/aaer/700-1400kw/a-1000s/>
- [31] J. Marriott, E. Sorensen, A general approach to modeling membrane modules, *Chem. Eng. Sci.* 58 (2003) 4975–4990.
- [32] C.J. Geankoplis, *Transport Processes and Unit Operations*, Prentice-Hall International, New Jersey, Ch. 13, 1993.
- [33] T.K. Sherwood, P.L.T. Brian, R.E. Fisher, P.K. Tewari, Desalination by reverse osmosis, *Ind. Eng. Chem. Fundam.* 6(1) (1967) 2–12.
- [34] R. Rautenbach, Process design and optimization, in: P.M. Bungay, H.K. Lonsdale, M.N. de Pinho (Eds.), *Synthetic Membranes: Science, Engineering and Applications*, Kluwer, New York, 1986.
- [35] P. Sarkar, D. Goswami, S. Prabhakar, P.K. Tewari, Optimized design of a reverse osmosis system with a recycle, *Desalination* 230 (2008) 128–139.
- [36] S.P. Agashichev, Reverse osmosis at elevated temperatures; influence of temperature on degree of concentration polarization and transmembrane flux, *Desalination* 179 (2005) 61–72.
- [37] A.R. Da Costa, A.G. Fane, D.E. Wiley, Spacer characterization and pressure drop modelling in spacer-filled channels for ultrafiltration, *J. Membr. Sci.* 87 (1994) 79–98.
- [38] N. Al-Bastaki, A. Abbas, Permeate recycle to improve the performance of a spiral-wound RO plant, *Desalination* 158 (2003) 119–126.
- [39] S. Sourirajan, *Reverse Osmosis*, Academic Press, New York, 1970.
- [40] Z. Amor, S. Malki, M. Taky, B. Bariou, N. Mameri, A. Elmidaoui, Optimization of fluoride removal from brackish water by electro dialysis, *Desalination* 120 (1998) 263–271.
- [41] G. Schock, A. Miquel, Mass transfer and pressure loss in spiral wound modules, *Desalination* 64 (1987) 339–352.
- [42] M. Abbas, B. Boumeddane, N. Said, A. Chikouche, Techno economic evaluation of solar dish Stirling system for stand-alone electricity in Algeria, *J. Eng. Appl. Sci.* 4 (2009) 258–267.
- [43] D. Zejli, R. Benchrifia, A. Bennouna, K. Zazi, Economic analysis of wind powered desalination in the south of Morocco, *Desalination* 165 (2004) 219–230.
- [44] D. Voivontas, K. Misirlis, E. Manoli, G. Arampatzis, D. Assimacopoulos, A tool of the design of desalination plant powered by renewable energies, *Desalination* 133 (2001) 175–198.
- [45] Y. Himri, A.S. Malik, A. Boudghene Stambouli, S. Himri, B. Draoui, Review and use of the Algerian renewable energy for sustainable development, *Renewable and Sustainable Energy Rev.* 13 (2009) 1584–1591.
- [46] D. Zouini, Le dessalement de l'eau de mer par osmose inverse: Une solution pour l'alimentation en eau des villes côtières de l'Algérie [Seawater desalination by reverse osmosis: An alternative water supply for coastal cities of Algeria], *Revue HTE*, No. 142, 2009, pp. 78–86.
- [47] E. Mary, Clayton et al., Implementation of brackish groundwater desalination using wind-generated electricity as a proxy for energy storage: A case study of the energy-water nexus in Texas, *Proceedings of the 12th International Mechanical Engineering Congress & Exposition*, Colorado, USA, November 11–17, 2011.
- [48] M. Wilf, K. Klinko, Optimization of seawater RO systems design, *Desalination* 138 (2001) 299–306.

- [49] J.A.G.C.R. Pais, L.M. Gando-Ferreira, Estimation in reverse osmosis seawater desalination, *Desalin. Water Treat.* 1 (2009) 82–87.
- [50] A. Zhu, P.D. Christofides, Y. Cohen, Minimization of energy consumption for a two-pass membrane desalination: Effect of energy recovery membrane rejection and retentate recycling, *J. Membr. Sci.* 339 (2009) 126–137.
- [51] S.A. Avlonitis, D.A. Avlonitis, T.H. Panagiotidis, Experimental study of the specific energy consumption for brackish water desalination by reverse osmosis, *Int. J. Energy Res.* 36 (2012) 36–45.
- [52] A. Abbas, Simulation and analysis of an industrial water desalination plant, *Chem. Eng. Process.* 44 (2005) 999–1004.